Predicting sudden stratospheric warming 2018 and its climate impacts with a multi-model ensemble

Geophysical Research Letters

RESEARCH LETTER
10.1029/2018GL081091

Special Section:
Bridging Weather and Climate: Subseasonal-to-Seasonal (S2S) Prediction

Predicting Sudden Stratospheric Warming 2018 and Its Climate Impacts With a Multimodel Ensemble

Alexey Yu. Karpechko[1], Andrew Charlton-Perez[2], Magdalena Balmaseda[3], Nicholas Tyrrell[1], and Frederic Vitart[3]

[1]Finnish Meteorological Institute, Helsinki, Finland, [2]Department of Meteorology, University of Reading, Reading, UK, [3]European Centre for Medium-Range Weather Forecasts, Reading, UK

Key Points:
- Subseasonal multimodel ensemble predicted increased odds of a large sudden stratospheric warming in February 2018 at a lead time of 11 days
- Extended cold anomaly over Eurasia in February 2018 was predicted more than 2 weeks ahead, but its intensity varied among individual models
- Accurate forecasting of a Ural high and associated upward wave activity flux are essential for improved prediction of stratospheric warming

Supporting Information:
- Supporting Information S1

Correspondence to:
A. Y. Karpechko,
alexey.karpechko@fmi.fi

Citation:
Karpechko, A. Y., Charlton-Perez, A., Balmaseda, M., Tyrrell, N., & Vitart, F. (2018). Predicting sudden stratospheric warming 2018 and its climate impacts with a multimodel ensemble. *Geophysical Research Letters*, *45*, 13,538–13,546. https://doi.org/10.1029/2018GL081091

Received 25 OCT 2018
Accepted 6 DEC 2018
Accepted article online 10 DEC 2018
Published online 26 DEC 2018

Abstract Sudden stratospheric warmings (SSWs) are significant source of enhanced subseasonal predictability, but whether this source is untapped in operational models remains an open question. Here we report on the prediction of the SSW on 12 February 2018, its dynamical precursors, and surface climate impacts by an ensemble of dynamical forecast models. The ensemble forecast from 1 February predicted 3 times increased odds of an SSW compared to climatology, although the lead time for SSW prediction varied among individual models. Errors in the forecast location of a Ural high and underestimated magnitude of upward wave activity flux reduced SSW forecast skill. Although the SSW's downward influence was not well forecasted, the observed northern Eurasia cold anomaly following SSW was predicted, albeit with a weaker magnitude, due to persistent tropospheric anomalies. The ensemble forecast from 8 February predicted the SSW, its subsequent downward influence, and a long-lasting cold anomaly at the surface.

Plain Language Summary Predicting climate anomalies more than 2 weeks ahead remains a challenging task. However, there are periods when climate is more predictable. In particular, it is known that in the wintertime Northern Hemisphere midlatitudes, climate may be more predictable during several weeks following sudden stratospheric warmings (SSWs), when a cold stratospheric polar vortex suddenly breaks and the stratosphere warms. In this article we evaluate quality of monthly forecasts by several up-to-date forecast systems during a sudden stratospheric warming observed in February 2018 focusing both on predictability of the stratospheric anomalies and on predictability of their surface impacts. We find that models predicted enhanced probability of sudden stratospheric warming at least 11 days before the observed event. Four days before the event it was forecast by all models with a very high certainty. We further show that successful prediction of the SSW required correct forecasting of anticyclonic anomaly over Ural and associated upward propagation of planetary-scale atmospheric waves. The observed cold anomaly across Eurasia in February 2018 was predicted more than 2 weeks ahead although at this lead time the predictability was more likely associated with persistence of tropospheric anomalies in the forecast, with smaller downward influence of the stratospheric anomalies.

1. Introduction

Major sudden stratospheric warmings (SSWs), or midwinter episodes of reversal of stratospheric westerly winds, are often followed by periods of anomalous surface weather, in particular, cold air outbreaks in the densely populated regions of western Europe, Far East, and eastern United States (Garfinkel et al., 2017; Kolstad et al., 2010; Kretschmer et al., 2018; Lehtonen & Karpechko, 2016; Thompson et al., 2002). These episodes are driven by the stratosphere-troposphere dynamical coupling (Kidston et al., 2015). The long time scale of extratropical stratospheric variability in winter, on the order of 4–8 weeks (Baldwin et al., 2003) thus provide an opportunity for predicting surface anomalies at longer lead times than is usually possible in the midlatitudes (Charlton et al., 2003; Christiansen, 2005; Karpechko, 2015; Sigmond et al., 2013; Tripathi et al., 2015).

The most recent major SSW occurred during February 2018. The onset date was 12 February 2018, defined as the first date when zonal mean zonal wind at 10 hPa and 60°N (U10) reverse from westerly to easterly (see Figure 1). This SSW is the first major midwinter SSW that occurred after establishment of the international subseasonal to seasonal forecasts (S2S) database (Vitart et al., 2017) and so represents an excellent early opportunity to study the ability of S2S models to predict SSW events and their surface impact. The SSW also receives special attention because of its possible association with the intense cold spell over Eurasia during

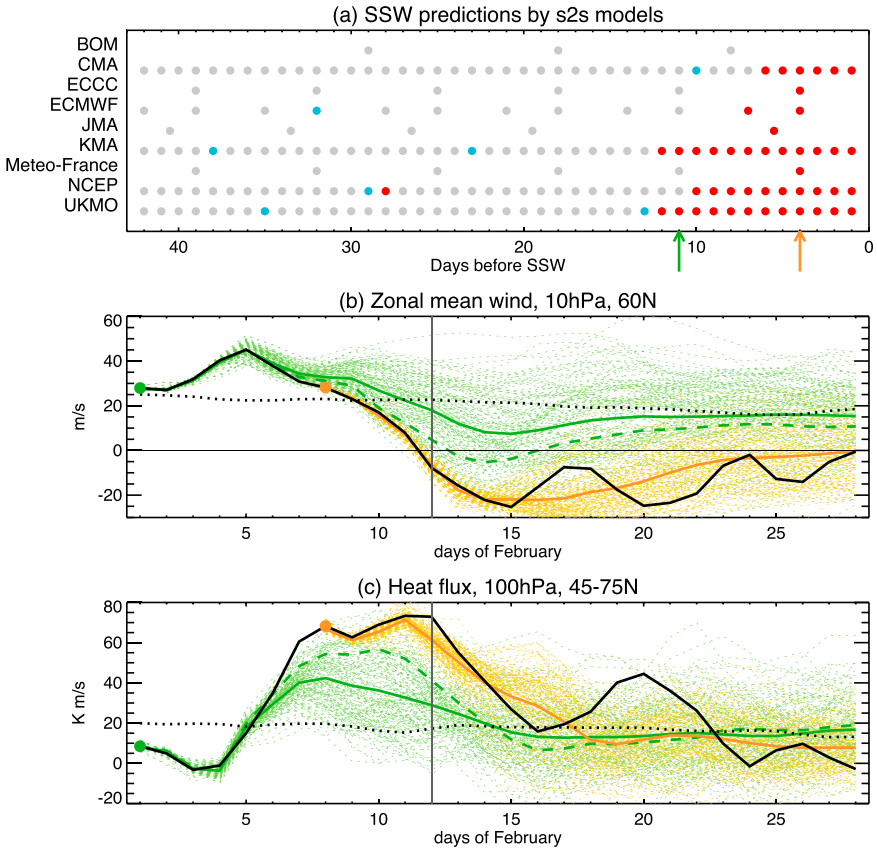

Figure 1. (a) Predictions of sudden stratospheric warming (SSW) 2018, defined as the first day when the ensemble mean predicted U10 became negative, by individual s2s models. Red dots indicate that an SSW is predicted within 3 days from the actually observed event. Blue dots indicate that an SSW is predicted on a different date than the actual event. Gray dots indicate that no SSW is predicted. Arrows point to forecasts used in the multimodel ensembles. (b) Time series of U10. Colored solid lines are multimodel means and dotted lines are ensemble members. Forecasts from 1 February 2018 are in green, forecasts from 8 February are in orange. Dashed green line shows U10 averaged over 10% of ensemble members with the largest SLP anomaly over southern Ural region indicated in Figure 2. Solid black line shows ERA-I U10 in 2018. Dotted black line shows ERA-I climatology. Vertical line marks SSW onset date. (c) The same as in (b) except for eddy heat flux at 100 hPa and averaged across 45–75°N.

late February to March 2018. This paper will investigate both the prediction of the SSW and the cold anomalies and elucidate their relation. Tripathi et al. (2016) were the first to apply a multimodel ensemble of five numerical weather prediction models to investigate predictability of an SSW; however, they did not look into the predictability of the following climate impacts. Thus, our study is the first to use an ensemble of subseasonal forecast models to investigate predictability of both an SSW and its climate impacts. Furthermore, the ensemble we use is made up of models explicitly designed to produce forecasts on subseasonal time scales.

2. Data and Methods

We use forecasts from the subseasonal to seasonal (S2S) database (Vitart et al., 2017, data available from s2s.ecmwf.int). This database is updated in a near real time, with a delay of approximately 3 weeks. Individual models used in this study as well as their forecast ensembles are described in Table S1 in the supporting information. In short, we analyze available forecasts by nine S2S models whose ensemble sizes range from 51 members (ECMWF, Meteo-France) to 4 members (CMA, KMA, UKMO). For forecast verification, we use ECMWF's reanalysis ERA-Interim (ERA-I; Dee et al., 2011).

Stratospheric winds and meridional eddy heat flux are analyzed as full fields, while all other variables are analyzed as anomalies. To make multimodel ensembles of forecast anomalies, the anomalies are first

calculated for each model with respect to the model's own climatologies. Model climatologies are calculated as averages over all available historical forecasts, which for each model are available for different periods (see Table S1). ERA-I anomalies are calculated with respect to the period 1981–2010. To assess the possible influence of differences in the periods used for defining climatology between ERA-I and models, the calculations were repeated with ERA-I climatology defined over the period 1996–2010, which largely overlaps with the periods used for most S2S models. The differences were found to be minimal (not shown) reassuring that our results are insensitive to the definition of climatology. In our approach, multimodel ensembles are formed from individual ensemble members, and therefore, different models have different weight in multimodel mean (MMM) proportional to their number of ensemble members (the pooled ensemble method is discussed by Weigel et al., 2008). This is different from an approach in which MMMs are made by combining model means. Our approach has the benefit of preserving ensemble spread and having larger ensemble size. In total, our multimodel ensembles consist of 151 members.

3. Results

3.1. SSW and Its Dynamical Precursors

We start by demonstrating the predictability of the SSW by the multimodel ensemble. Figure 1a summarizes the predictability of the SSW as a function of lead time for each model. Here the SSW is considered to be predicted when the ensemble mean U10 turns negative within 3 days from the actual event. Note that different models produce forecasts with different frequency; therefore, direct comparison of predictability between the models is challenging. Nevertheless, two time slices taken when forecasts are simultaneously available from most of the models provide a good overview of the SSW predictability by the ensemble. In forecasts from 1 February 2018, only two models, UKMO and KMA, predict an SSW. These same models also predict the SSW in forecasts from 31 January 2018, that is, 13 days before the observed event. In contrast, all seven models that provide forecasts on 8 February 2018, predict an SSW. In the following text, we will analyze the forecasts from 1 to 8 February 2018. For two models, JMA and BoM, the forecasts are not available on either 1 or 8 February 2018. For consistency we do not consider these models in the rest of the manuscript. Note that JMA predicted the SSW in their forecast from 6 February 2018, while BoM did not predict the SSW in their forecast from 4 February 2018. The latter model has very coarse resolution in the stratosphere and therefore it is not expected to be able to resolve stratospheric processes.

Figure 1b shows the evolution of the observed and forecast U10 during February 2018. Forecasts from 1 February 2018 show a weakening of the winds after 4 February 2018. However, the magnitude of the weakening in the MMM is underestimated and the MMM does not become negative. In both forecast and observations, minimum U10 is achieved on 15 February 2018 when the ensemble mean forecast value is 7 m/s compared with observed −25 m/s. Defining the forecast daily SSW probability as the fraction of ensemble members predicting easterlies on that day (Karpechko, 2018; Taguchi, 2016; Tripathi et al., 2016), we find that the forecast SSW probability peaks on 15 February when it reaches 0.33. The climatological frequency of easterlies on any February day is 0.11, which we find in S2S hindcasts, suggesting that the multimodel ensemble predicts that the odds of an SSW have increased by 3 times compared to model's climatology. This is consistent with the fact that some models (UKMO and KMA) predict an SSW even in their ensemble mean. Looking at the forecasts from 8 February 2018 one can see that the models correctly predict the onset date of the SSW occurrence when its forecasted probability reaches 0.99. The ensemble from 8 February also predicts the long recovery from SSW in the stratosphere with the MMM U10 remaining negative through February as observed. The average spread of the multimodel ensemble is also smaller during weeks 3 and 4 for the forecasts initialized on 8 February compared to the forecasts from 1 February.

Figure 1c shows forecasts of the zonal mean meridional eddy heat flux at 100 hPa, which is a proxy for the wave forcing of the stratospheric circulation. In forecasts from 1 February 2018, all ensemble members predict an increase in the heat flux with respect to climatology; however, the magnitude of the increase is strongly underestimated when compared with observations. In the MMM, the heat flux maximizes on 7 and 8 February 2018 at 42 $K{\cdot}m{\cdot}s^{-1}$, while the observed heat flux peaks on 11 February 2018 at 73 $K{\cdot}m{\cdot}s^{-1}$. The mean eddy heat flux averaged over the period before the SSW (1 to 11 February 2018) strongly correlates with forecast U10 on 12 February across ensemble members ($r = 0.94$). The time-averaged MMM heat flux over this period in only 22 $K{\cdot}m{\cdot}s^{-1}$, which is 1.6 times less than the observed value of 36 $K{\cdot}m{\cdot}s^{-1}$. When

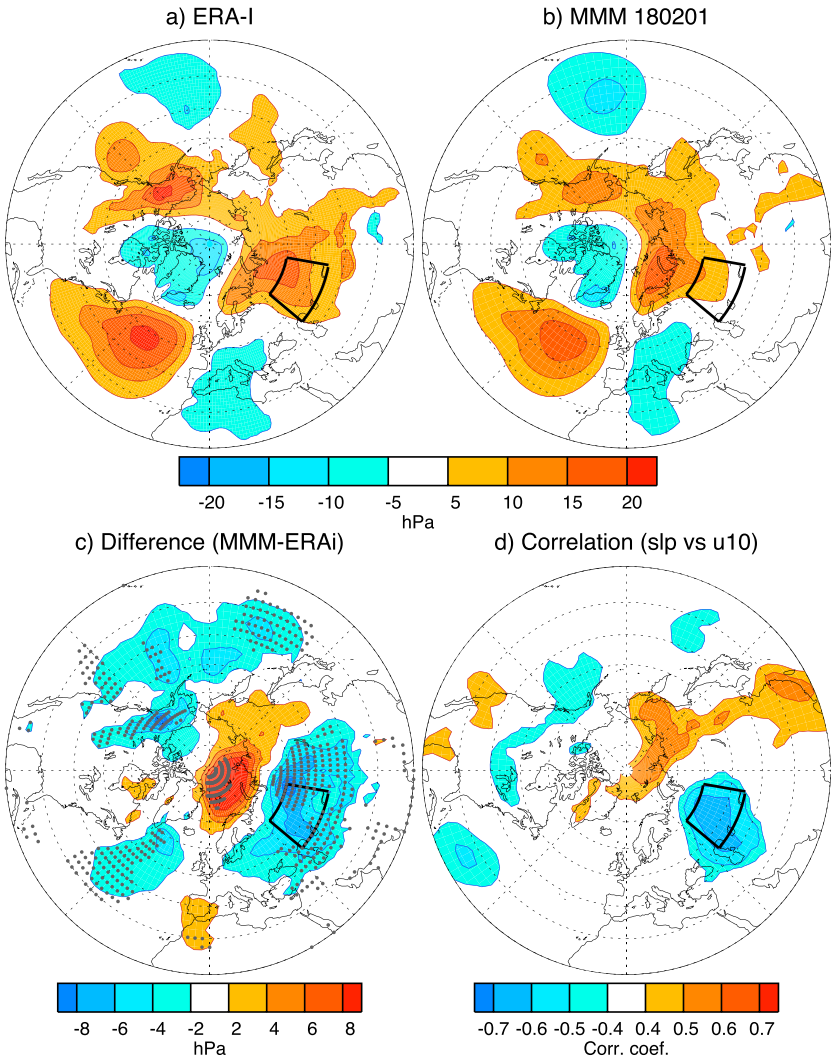

Figure 2. Sea level pressure anomalies averaged during 1–11 February 2018. (a) ERA-I; (b) MMM forecast from 1 February. (c) Difference between (b) and (a). (d) Correlation coefficient between sea level pressure forecasts averaged during 1–11 February and U10 forecasts valid on 12 February 2018 across individual ensemble members. Dots in (c) show where observed anomaly is outside the 10–90% range across forecast members. All coefficients shaded in (d) are significant at $p = 0.01$. Black contours mark southern Ural region used for forecast subsampling (see the text for more details).

the heat flux is averaged only across the ensemble members predicting the SSW, the result is 32 K·m·s^{-1}, in better agreement with observations, with some individual ensemble members reaching the observed value. In the forecast from 8 February, the initial eddy heat flux was very large (~65 K·m·s^{-1}), and its subsequent evolution was well predicted by the MMM, consistent with the forecast of the SSW by this ensemble.

We next look at tropospheric precursors of SSW. Figure 2 shows mean SLP anomalies averaged over the period 1 to 11 February 2018 in ERA-I and in the forecasts from 1 February 2018. Both observed (Figure 2a) and forecast (Figure 2b) fields show three anomalous highs—over the North Atlantic, Ural Mountains, and Alaska. Blocking anticyclones in these regions were earlier associated with tropospheric forcing of SSWs (Cohen & Jones, 2011; Garfinkel et al., 2010; Martius et al., 2009; Woollings et al., 2010). Martius et al. (2009) associated splitting SSWs, that is, the type that occurred in February 2018 (not shown), with blocks appearing either over the Pacific region, or over both Pacific and Euro-Atlantic regions simultaneously. Looking at Figure 2, the forecasted field appears remarkably similar to the observed one; however, closer comparison reveals important differences (Figure 2c). In particular, the Ural high is shifted northward by ~10° in the forecast and also extends further east in comparison to the observed one, which is evident from the dipole of positive and

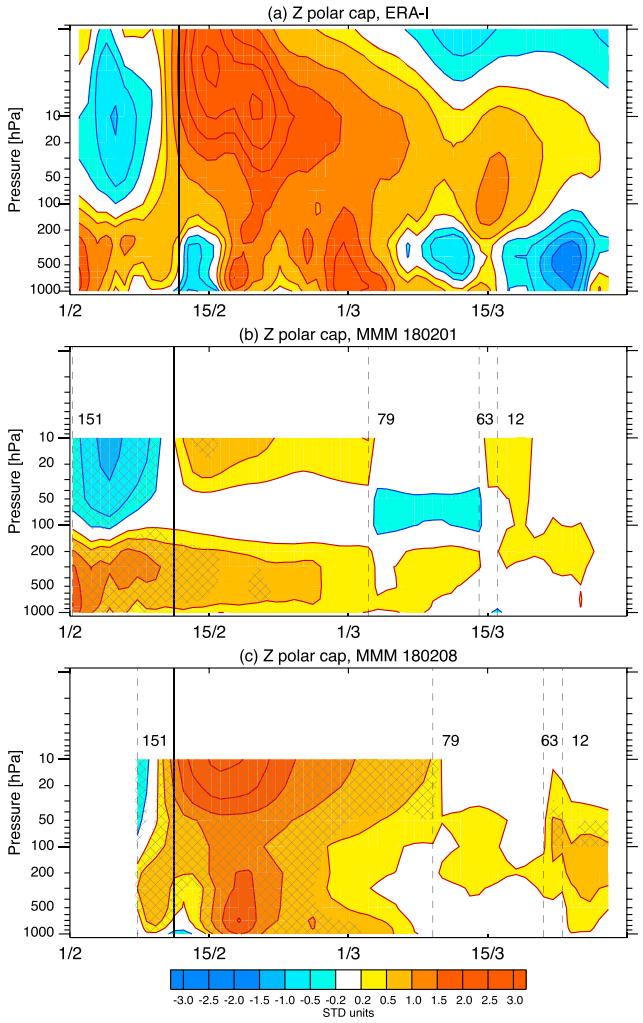

Figure 3. Evolution of the normalized geopotential height anomalies averaged over polar cap (60–90°N) between 1 February and 31 March 2018. (a) ERA-I; (b) MMM forecast from 1 February; (c) MMM forecast from 8 February 2018. Hatching indicates that ≥75% of ensemble members agree on the sign of the anomalies.

negative differences in the Siberian sector (Figure 2c). To relate forecasts of SLP to forecasts of SSW, we correlate SLP anomalies averaged over 1 to 11 February at each grid point with U10 forecasts valid on 12 February across ensemble members (e.g., Tripathi et al., 2016). Before calculating the correlations, for each ensemble member, we first remove respective single-model ensemble mean U10 and SLP anomaly at each grid point. This procedure, which is applied to exclude the influence of individual model biases, results in somewhat higher magnitude of the correlation coefficients (approximately by 0.1); however, this does not change considerably the spatial structure. Over Siberia, the correlation field (Figure 2d) resembles the differences between the observed and forecasted SLP with statistically significant negative correlation coefficients exceeding −0.6 in the southern Ural, where the magnitude of the observed anomaly is underestimated by the forecasts, and also with positive coefficients in northeast Siberia where the magnitude of the forecasted anomalies is overestimated. Thus, the correlations field indicates that stronger SLP is southern Ural is associated with weaker stratospheric winds and suggests that errors in the location of the Ural high turn out to be crucial for forecasting SSW. To confirm this result we subselect 10% of the ensemble members with the largest positive SLP anomaly in southern Ural and find that the average across this subgroup predicts an SSW to occur on 13 February 2018 together with a larger eddy heat flux in comparison to that in the full ensemble (Figures 1b and 1c). Note that there are errors in the forecasted magnitude of the Alaska high too (Figure 2c); however, they are not well correlated to the stratospheric forecast across the ensemble for this event (Figure 2d). Note also that the forecast errors as well as correlations patterns between SLP and stratospheric winds are largely similar across individual models (Figure S1).

3.2. Downward Propagation and Surface Impacts

It is well known that stratospheric zonal mean circulation anomalies tend to propagate downward and often affect tropospheric and surface climate. Figure 3 shows normalized geopotential height anomalies averaged over 60–90°N (Z) during February and March 2018. This diagnostic is widely used to illustrate stratosphere-troposphere coupling, and it strongly correlates (r ~ 0.9) with other indices used to represent the Northern Annular Mode (Baldwin & Dunkerton, 1999; Karpechko et al., 2017; Runde et al., 2016). In observations, significant positive anomalies develop in the upper stratosphere during the onset of the SSW, indicating a weakening of the polar vortex. The large negative annular mode anomaly propagates downward with time through the stratosphere and persists in the lower stratosphere for several weeks from mid-February until the second half of March, as is often observed during SSW events (Hitchcock et al., 2013). In the troposphere there are several episodes of positive Z anomalies—one in mid-February soon after the SSW and another one in the beginning of March.

The forecasts from 1 February 2018 reproduce the observed significant positive anomalies in the middle stratosphere above 30 hPa after SSW (Figure 3b); however, the ensemble mean anomalies last only for several days and do not propagate to the lower stratosphere as observed. Interestingly, despite the lack of a downward propagation, the observed positive Z anomalies in the troposphere are predicted by the MMM until mid-March, and the ensemble members show remarkable agreement, with >75% of ensemble members agreeing on the sign of the anomaly, until the second half of February, that is, beyond the typical weather predictability horizon. Figure 3b suggests that persistence of tropospheric anomalies represents the source of forecast skill in this case, although the downward influence forecasted by a fraction of ensemble members has likely contributed to the skill. (Note that there is an apparent discontinuity in the forecasted anomalies in Figure 3, which occurs because for some models the forecasts are not available for the whole analysis period).

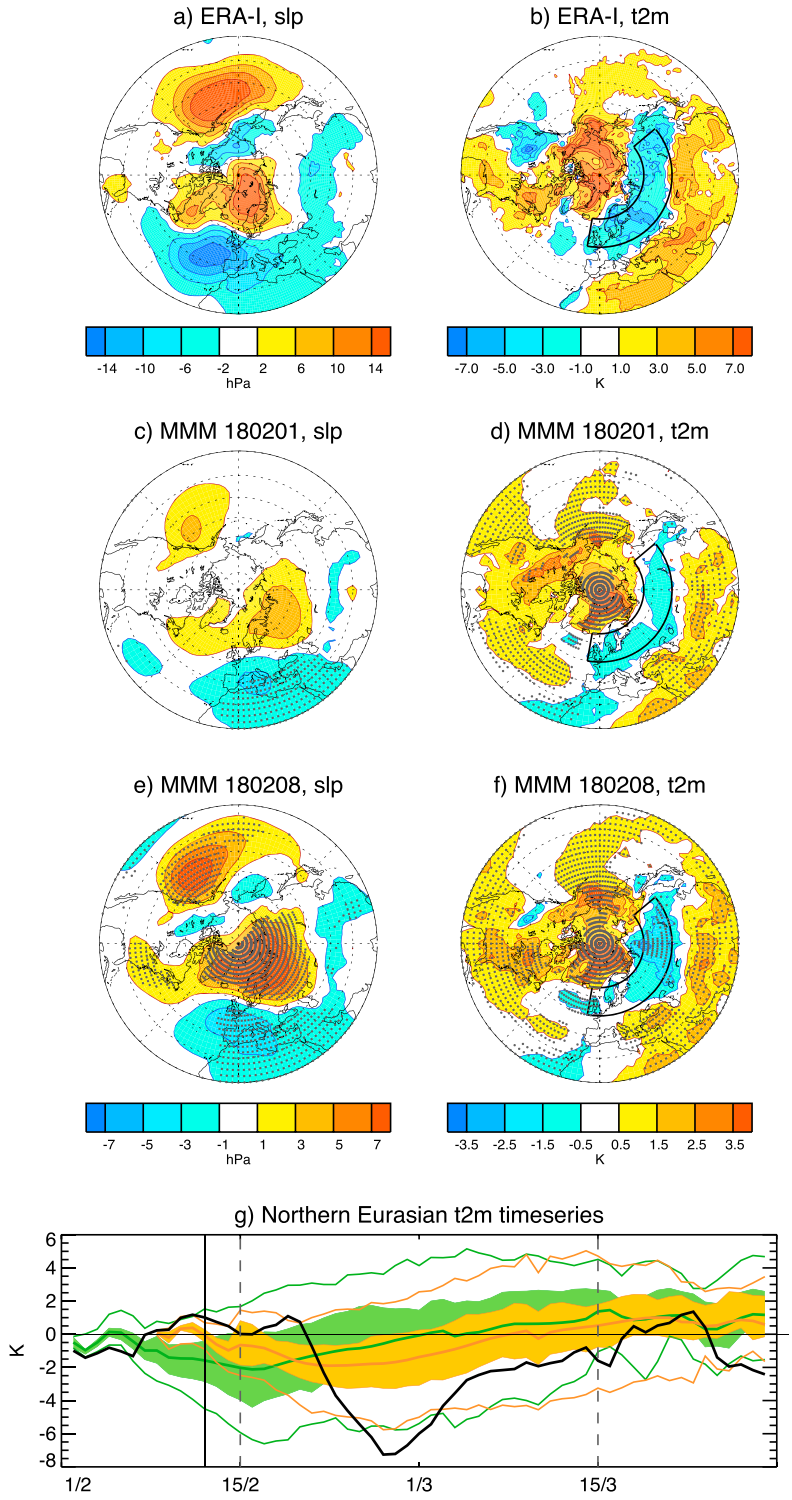

Figure 4. (a, c, and e) Sea level pressure anomalies averaged over the 30-day period starting from 15 February 2018. (a) ERA-Interim; (c) Multimodel mean forecast from 1 February; (e) Multimodel mean forecast from 8 February 2018. Dots in (c) and (e) show where ≥75% of ensemble members agree on anomaly sign. (b, d, and f) The same as in (a), (c), and (e) except for 2-m temperature anomalies. (g) Time series of the forecasted (colored lines) and ERA-I (black line) 2-m temperatures averaged over northern Eurasia region indicated in (b), (c), (d). Green (orange) lines show forecasts from 1 February (8 February). Thick colored lines show MMM forecasts; shaded regions show 25th to 75th percentiles and thin colored lines show 5th to 95th percentiles. Solid vertical line marks sudden stratospheric warming onset date. Dashed vertical lines mark period used for averaging anomalies in (a)–(f).

Table 1
Observed and Forecasted by Multimodel Ensembles Temperature Anomaly (°C) Averaged over 50°N–65°N and 10°W–130°E

	ERA-interim	Mean forecast from 1 February 2018	Mean forecast from 8 February 2018
15 February to 16 March	−2.71	−0.62	−1.00
22 February to 16 March	−3.62	−0.11	−0.95

Turning to the forecast from 8 February 2018 when the multimodel ensemble successfully predicted SSW, one can see that the ensemble captures the observed downward propagation of the anomalies as well as their long duration in the lower stratosphere during the SSW recovery phase. The MMM does not reproduce the observed temporal variability in the troposphere with its periods of strengthening and weakening of the Z anomalies. However, several models do capture the timing of the two major episodes of positive Z anomalies (Figure S2), which suggests that even individual stratosphere-troposphere coupling episodes may be predictable beyond 2 weeks.

Cold anomalies observed after SSWs are a well-known example of the stratospheric influence on weather. Although the largest anomalies usually occur in Northern Siberia (Butler et al., 2017; Thompson et al., 2002), cold outbreaks are also observed across Europe where the potential impact of extreme weather is greater due to the higher density of population and infrastructure. Figures 4a an 4b shows observed SLP and 2-m temperature anomalies averaged over the 30-day period starting from 15 February 2018, that is, covering the period of stratosphere-troposphere coupling events (Figure 3). The SLP field is characterized by mostly positive anomalies over the polar cap, consistent with observed Z anomalies (Figure 3a). In the Euro-Atlantic sector, there is a pronounced dipole pattern indicative of a negative phase of the North Atlantic Oscillation. Such a configuration of SLP anomalies suggests an advection of the cold Siberian air mass toward Europe. Consistently, significant cold anomalies are observed extending from UK toward the Far East between 45°N and 70°N. Looking first at the forecast from 1 February, one can see similar cold anomalies although with a much weaker magnitude (Figure 4d and Table 1). In this forecast, the observed downward propagation is not captured, and thus a stratospheric influence is not well predicted by the MMM (Figure 3b). The predicted cold anomalies are associated with a positive SLP anomaly seen over Northwestern Russia which is shifted further south in comparison to the observed anomaly (Figure 4c). Figure 4g shows that the forecasted cold anomaly over northern Eurasia starts earlier than in observations and ends before March, also earlier than observed. The forecast initialized from 8 February also underestimates the magnitude of the cold anomaly when compared to observations (Figure 4f, Table 1); however, in this case, the timing of the cold spell is in better agreement with observations (Figure 4g) and the spatial structures of the anomalies, as measured by anomaly correlation coefficients (ACC), are better captured (Figures 4e and 4f, Table S2). Note that the magnitude of the forecasted 2-m temperature anomaly is comparable between the averaging periods starting from 15 February 2018 and a week later (from 22 February), which is likely because this ensemble captures the delayed downward influence of the stratospheric anomalies (Figure 3c). Note that the cold spell is also predicted by most individual models from both forecast dates (Figures S3 and S4 and Table S2); however, the MMM overperforms or shows comparable skill to the best individual model in terms of ACC, which is a well-known effect on seasonal-scale forecasting (e.g., Weigel et al., 2008 and references therein).

4. Discussion and Conclusions

In this study we, for the first time, applied a multimodel ensemble of subseasonal forecasts to study dynamical evolution of an SSW and its surface impacts. Our study highlights the success of this ensemble in predicting surface climate anomalies following the SSW over the period of about 1 month, that is, beyond the weather predictability horizon in the extratropics. Earlier it was demonstrated that state-of-the-art forecast systems are capable of capturing downward propagation and surface impacts of stratospheric anomalies contributing to skillful subseasonal forecasts (Sigmond et al., 2013; Tripathi et al., 2015). Here we show that skillful forecasts are possible as soon as the models start to predict SSW, or at least 4 days before the onset date. We have also shown that the limiting factor in predicting the SSW itself at lead time of about 10 days was an underestimation of the magnitude of wave activity propagation to the stratosphere linked in turn to errors in the location of an Ural high. An underestimated magnitude of forecasted wave activity flux was earlier pointed by Taguchi (2016) and the link to forecasted SLP anomalies over northern Europe was pointed by Tripathi et al. (2016) in their studies of other SSWs. It remains, however, unclear whether these errors are due to common biases across the models or because SSWs are associated with extreme dynamical evolutions located at, or beyond, the tails of forecast ensembles. More comprehensive investigation of historical forecasts and longer runs of climate models may help in answering this question.

Another question unanswered in our study is how this SSW was related to remote forcing, such as the Madden-Julian oscillation (MJO). An MJO of large magnitude was observed in January 2018 before the SSW and in principle could have forced an SSW (e.g., Garfinkel & Schwartz, 2017). It is possible that ensemble members more accurately predicting the MJO would also be more successful in predicting SSW (Garfinkel & Schwartz, 2017). A brief analysis of forecasts by one of the models (ECMWF) did not show a link between forecasts of MJO and SSW; however, more research is needed to understand the relationship between the MJO, SSW, and extratropical surface anomalies. In particular, it is possible that the effect of the MJO on the extratropical troposphere could have been captured by the ensemble and thus provided the demonstrated skill to the forecasts in the troposphere, already at lead time of 11 days when the SSW has not yet been predicted by most of the models. Similarly, the success of the models in simulating the SSW could also be linked to their ability to accurately capture the MJO and its teleconnections.

We conclude by pointing to the benefit of using multimodel ensembles, which have a long history in climate change research and seasonal forecasting, for analyzing subseasonal climate variability. Models have different strengths and weakness. For example, the UKMO and KMA models appear successful at predicting the SSW, and they show a strong connection between a weak polar vortex and following SLP anomalies; however, this connection does not necessary lead to improved predictions of near-surface temperatures. Other models, like ECMWF, have a weak connection between the polar vortex and SLP, but they show good forecast of near-surface temperature, probably because of the initialization of land conditions. These multimodel results suggest that there is room for gaining predictive skill of these extreme cold spells by improving these aspects in the respective models. In the meantime, the multimodel ensemble is a pragmatic approach for combining the strengths of the different forecasting systems. Using such ensemble could be useful especially at long lead times when signal-to-noise ratio is weak and multimodel ensembles have the benefit of both increasing the size of ensemble and canceling out systematic biases of individual models. Averaging across the model ensemble also helps to isolate particularly interesting features of the atmospheric flow linked to stratosphere-troposphere coupling. Our study provides an example of how such ensembles can be utilized for studying stratosphere-troposphere coupling.

Acknowledgments

A. Y. K. and N. T. are funded by the Academy of Finland (grants 286298, 294120, and 319397). A. J. C. P. performed the work in this study while on sabbatical at the European Centre for Medium-Range Weather Forecasts. We thank two anonymous reviewers for their helpful comments. This work is based on S2S data. S2S is a joint initiative of the World Weather Research Programme (WWRP) and the World Climate Research Programme (WCRP). The original S2S database is hosted at ECMWF as an extension of the TIGGE database and is available from s2s.ecmwf.int.

References

Baldwin, M. P., & Dunkerton, T. J. (1999). Propagation of the Arctic oscillation from the stratosphere to the troposphere. *Journal of Geophysical Research*, *104*, 30, 937–30, 946. https://doi.org/10.1029/1999JD900445

Baldwin, M. P., Stephenson, D. B., Thompson, D. W. J., Dunkerton, T. J., Charlton, A. J., & O'Neill, A. (2003). Stratospheric memory and skill of extended-range weather forecasts. *Science*, *301*(5633), 636–640. https://doi.org/10.1126/science.1087143

Butler, A. H., Sjoberg, J. P., Seidel, D. J., & Rosenlof, K. H. (2017). A sudden stratospheric warming compendium. *Earth System Science Data*, *9*(1), 63–76. https://doi.org/10.5194/essd-9-63-2017

Charlton, A. J., O'Neill, A., Stephenson, D. B., Lahoz, W. A., & Baldwin, M. P. (2003). Can knowledge of the state of the stratosphere be used to improve statistical forecasts of the troposphere? *Quarterly Journal of the Royal Meteorological Society*, *129*(595), 3205–3224. https://doi.org/10.1256/qj.02.232

Christiansen, B. (2005). Downward propagation and statistical forecast of the near-surface weather. *Journal of Geophysical Research*, *110*, D14104. https://doi.org/10.1029/2004JD005431

Cohen, J., & Jones, J. (2011). Tropospheric precursors and stratospheric warmings. *Journal of Climate*, *24*(24), 6562–6572. https://doi.org/10.1175/2011JCLI4160.1

Dee, D. P., Uppala, S. M., Simmons, A. J., Berrisford, P., Poli, P., Kobayashi, S., et al. (2011). The ERA-interim reanalysis: Configuration and performance of the data assimilation system. *Quarterly Journal of the Royal Meteorological Society*, *137*(656), 553–597. https://doi.org/10.1002/qj.828

Garfinkel, C. I., Hartmann, D. L., & Sassi, F. (2010). Tropospheric precursors of anomalous northern hemisphere stratospheric polar vortices. *Journal of Climate*, *23*(12), 3282–3299. https://doi.org/10.1175/2010JCLI3010.1

Garfinkel, C. I., & Schwartz, C. (2017). MJO-related tropical convection anomalies lead to more accurate stratospheric vortex variability in subseasonal forecast models. *Geophysical Research Letters*, *44*, 10,054–10,062. https://doi.org/10.1002/2017GL074470

Garfinkel, C. I., Son, S. W., Song, K., Aquila, V., & Oman, L. D. (2017). Stratospheric variability contributed to and sustained the recent hiatus in Eurasian winter warming. *Geophysical Research Letters*, *44*, 374–382. https://doi.org/10.1002/2016GL072035

Hitchcock, P., Shepherd, T. G., & Manney, G. L. (2013). Statistical characterization of Arctic polar-night jet oscillation events. *Journal of Atmospheric Science*, *26*(6), 2096–2116. https://doi.org/10.1175/JCLI-D-12-00202.1

Karpechko, A. Y. (2015). Improvements in statistical forecasts of monthly and bi-monthly surface air temperatures from stratospheric predictor. *Quarterly Journal of the Royal Meteorological Society*, *141*(691), 2444–2456. https://doi.org/10.1002/qj.2535

Karpechko, A. Y. (2018). Predictability of sudden stratospheric warmings in the ECMWF extended-range forecast system. *Monthly Weather Review*, *146*(4), 1063–1075. https://doi.org/10.1175/MWR-D-17-0317.1

Karpechko, A. Y., Hitchcock, P., Peters, D. H. W., & Schneidereit, A. (2017). Predictability of downward propagation of major sudden stratospheric warmings. *Quarterly Journal of the Royal Meteorological Society*, *143*(704), 1459–1470. https://doi.org/10.1002/qj.3017

Kidston, J., Scaife, A. A., Hardiman, S. C., Mitchell, D. M., Butchart, N., Baldwin, M. P., & Gray, L. J. (2015). Stratospheric influence on tropospheric jet streams, storm tracks and surface weather. *Nature Geoscience*, *8*(6), 433–440. https://doi.org/10.1038/ngeo2424

Kolstad, E. W., Breiteig, T., & Scaife, A. A. (2010). The association between stratospheric weak polar vortex events and cold air outbreaks in the northern hemisphere. *Quarterly Journal of the Royal Meteorological Society*, *136*(649), 886–893. https://doi.org/10.1002/qj.620

Kretschmer, M., Coumou, D., Agel, L., Barlow, M., Tziperman, E., & Cohen, J. (2018). More-persistent weak stratospheric polar vortex states linked to cold extremes. *Bulletin of the American Meteorological Society*, *99*(1), 49–60. https://doi.org/10.1175/BAMS-D-16-0259.1

Lehtonen, I., & Karpechko, A. Y. (2016). Observed and modeled tropospheric cold anomalies associated with sudden stratospheric warmings. *Journal of Geophysical Research: Atmospheres*, *121*, 1591–1610. https://doi.org/10.1002/2015JD023860

Martius, O., Polvani, L. M., & Davies, H. C. (2009). Blocking precursors to stratospheric sudden warming events. *Geophysical Research Letters*, *36*, L14806. https://doi.org/10.1029/2009GL038776

Runde, T., Dameris, M., Garny, H., & Kinnison, D. E. (2016). Classification of stratospheric extreme events according to their downward propagation to the troposphere. *Geophysical Research Letters*, *43*, 6665–6672. https://doi.org/10.1002/2016GL069569

Sigmond, M., Scinocca, J. F., Kharin, V. V., & Shepherd, T. G. (2013). Enhanced seasonal forecast skill following stratospheric sudden warmings. *Nature Geoscience*, *6*(2), 98–102. https://doi.org/10.1038/ngeo1698

Taguchi, M. (2016). Predictability of major stratospheric sudden warmings: Analysis results from JMA operational 1-month ensemble predictions from 2001/02 to 2012/13. *Journal of Atmospheric Science*, *73*(2), 789–806. https://doi.org/10.1175/JAS-D-15-0201.1

Thompson, D. W. J., Baldwin, M. P., & Wallace, J. M. (2002). Stratospheric connection to northern hemisphere wintertime weather: Implications for prediction. *Journal of Climate*, *15*(12), 1421–1428. https://doi.org/10.1175/1520-0442(2002)015<1421:SCTNHW>2.0.CO;2

Tripathi, O. P., Baldwin, M., Charlton-Perez, A., Charron, M., Cheung, J. C. H., Eckermann, S. D., et al. (2016). Examining the predictability of the stratospheric sudden warming of January 2013 using multiple NWP systems. *Monthly Weather Review*, *144*(5), 1935–1960. https://doi.org/10.1175/MWR-D-15-0010.1

Tripathi, O. P., Charlton-Perez, A., Sigmond, M., & Vitart, F. (2015). Enhanced long-range forecast skill in boreal winter following stratospheric strong vortex conditions. *Environmental Research Letters*, *10*(10), 104007. https://doi.org/10.1088/1748-9326/10/10/104007

Vitart, F., Ardilouze, C., Bonet, A., Brookshaw, A., Chen, M., Codorean, C., et al. (2017). The subseasonal to seasonal (S2S) prediction project database. *Bulletin of the American Meteorological Society*, *98*(1), 163–173. https://doi.org/10.1175/BAMS-D-16-0017.1

Weigel, A. P., Liniger, M. A., & Appenzeller, C. (2008). Can multi-model combination really enhance the prediction skill of probabilistic ensemble forecasts? *Quarterly Journal of the Royal Meteorological Society*, *134*(630), 241–260. https://doi.org/10.1002/qj.210

Woollings, T., Charlton-Perez, A., Ineson, S., Marshall, A. G., & Masato, G. (2010). Associations between stratospheric variability and tropospheric blocking. *Journal of Geophysical Research*, *115*, D06108. https://doi.org/10.1029/2009JD012742